Magazine of Civil Engineering

ISSN 2712-8172

journal homepage: http://engstroy.spbstu.ru/

DOI: 10.34910/MCE.110.6

Numerical shear of post-tensioned beams with inverted-U shaped reinforcements

M. Khatib* [a], ***Z. Abou Saleh*** [b], ***O. Baalbaki*** [c], ***Z. Hamdan*** [d]

[a] *ISSEA-Cnam Lebanon, Maurice Barres, Beirut, Lebanon*

[b] *Rafik Hariri University, Damour, Lebanon*

[c] *Beirut Arab University, Beirut, Lebanon*

[d] *Lebanese University, Beirut, Lebanon*

**E-mail: milad.khatib@isae.edu.lb*

Keywords: finite element model, 3D modeling, bonded post-tensioned beams, shear stress, inverted-U shaped reinforcements, stirrups reinforcements

Abstract. Previous works verified that, compared to conventional stirrups reinforcements (or closed stirrups reinforcements), the inverted-U shaped reinforcements improve the performance of the flat slabs in terms of failure mode and load capacity. The primary goal of this research was to investigate the numerical advantage of the inverted-U shaped reinforcements in reinforcing post-tension beams (PTB) over the conventional one as well as comparing the results with the ACI provision. Several experiments and numerical analyses were conducted in order to increase the shear strength capacity of reinforced concrete beams using different shear reinforcement systems. Recently, the system's ability to experimentally improve the shear capacity of bonded post-tensioned beams was explored. In this study, two types of post-tensioned beams were tested using a finite element program (ANSYS 16.0) to help investigate the influence of inverted-U shaped reinforcements on the shear behavior of bonded post-tensioned beams. The numerical results indicated that the limitation on the nominal of shear reinforcements for bonded pre-stressed concrete beams in the ACI 318-14 was too conservative. Good correlation was found between the experimental and the numerical results.

1. Introduction

In 1872, the principle of prestressing the concrete was applied by Jackson for the first time in United States [1]. Later, several experimental tests were conducted on the behavior of bonded and unbonded post-tensioned concrete members such as: Dunker (1985) [2], Garden and Hollaway (1997) [3], Abou Saleh and Suaris (2007) [4], Kang and al. (2015) [5], Ellobody and Bailey (2016) [6], Xue and al. (2019) [7], Khatib and Abou Saleh (2020) [8], and others.

Normally, prestressed concrete can be constructed in three different ways: pre-tensioned prestressed concrete, bonded post-tensioned (PT) prestressed concrete, and unbonded PT prestressed concrete as cited by Kang and al. (2015) [8].

Since it is difficult to pinpoint an exact date for the initial development of the finite element analysis, a method initiated from necessity in order to explain and predict complex elasticity and structural analysis problems in civil and aeronautical engineering, its development can be traced back to the work done by Hrennikoff [9] and Courant in the early 1940s [10]. Numerical and theoretical models were previously developed by other researchers to study the behavior of bonded and unbonded post-tensioned concrete members.

Khatib, M., Abou Saleh, Z., Baalbaki, O., Hamdan, Z. Numerical shear of post-tensioned beams with inverted-U shaped reinforcements. Magazine of Civil Engineering. 2022. 110(2). Article No. 11006. DOI: 10.34910/MCE.110.6

Many articles and researches have been published addressing the optimization of concrete structures such as: Hopkins (1956) [11], Kim and Christopoulos (2008) [12], Ellobody and Bailey (2009) [13], Huang and al. (2010) [14], Kim and Lee (2012) [15], Kulkarni A. and Bhusare V (2016) [16], Khatib and al. (2016) [17], Abdul-Razzaq and al. (2018) [18], and Khatib and al. (2018) [19]. The techniques of optimization play an important role in the design of structures. One of the most important purposes of optimization is finding the best solutions from which a designer can realize the highest benefits and advantages within the available resources.

Generally, the beams may have major possible modes of failure (flexural failure, diagonal tension and shear failure), cracking, deflection, bending, and shear as discussed by Hawkins and al. [20] and recently by Slowik [21].

According to ACI 318 [22], the shear strength (V_c) for concrete section (with effective web width (b_w) and distance from extreme compression fiber to centroid of prestressing steel (d_p)) provided by pre-stressed reinforced concrete members. It was calculated in function of: modification factor related to the unit weight of concrete; λ, concrete compressive strength; f'_c, factored shear force; V_u, and factored moment; M_u. The shear strength (V_c) can be the lesser of the following:

$$V_c = \left(0.6\lambda\sqrt{f'_c} + 700 \cdot \frac{V_u d_p}{M_u} \right) \cdot b_w \cdot d_p, \tag{1}$$

where $\frac{V_u d_p}{M_u} \geq 1.0;$

The shear force at flexure-shear cracking $V_{ci} = 0.6\sqrt{f'_c} \cdot b_w \cdot d_p + V_c + \frac{V_i M_{cr}}{M_{\max}},$ (2)

where V_i is the factored shear force at section due to externally applied loads occurring simultaneously, M_{cr} is the cracked moment and M_{max} is the maximum moment.

The cracked moment (M_{cr}) for the section was calculated in function of: inertia of the section (I), concrete compressive strength (f'_c), average prestress value after losses at centroid of cross concrete section (f_{pe}), with unfactored dead load stress (f_d) at distance (y_t) from centroidal axis of gross section, neglecting reinforcement, to extreme fiber in tension as follows: $M_{cr} = \left(\frac{I}{y_t} \right) \left(6\sqrt{f'_c} + f_{pe} - f_d \right).$

In addition, for web shear (V_{CW}) in prestressed concrete members:

$$V_{cw} = \left(3.5\sqrt{f'_c} + 0.3 f_{pc} \right) \cdot b_w \cdot d_p + V_p. \tag{3}$$

where f_{pc} is the compressive stress in concrete after all prestress losses at centroid of cross section, and V_p is the vertical component of effective prestress force at the cross section.

However, the above equations of shear strength should not be less than those of shear strength provided by reinforced concrete members with calculated distance from extreme compression fiber to centroid of longitudinal tension reinforcement (d). V_c can be the lesser of the following:

$$\left(1.9\lambda\sqrt{f'_c} + 2500 V_n \frac{d_p}{M_u} \right) \cdot b_w \cdot d, \tag{4}$$

$$\left(1.9\lambda\sqrt{f'_c} + 2500 \right) \cdot b_w \cdot d, \tag{5}$$

with limitation:

$$\left(2\lambda\sqrt{f'_c} \right) \cdot b_w \cdot d \leq V_c \leq \left(5\lambda\sqrt{f'_c} \right) b_w \cdot d.$$

1.1. Shear reinforcement types

The following different systems of reinforcement were explained in order to highlight the differences between the conventional shear reinforcement system and the proposed one.

In 1899, Ritter stated that stirrups resisted tension, not horizontal shear. He also suggested the design of vertical stirrups (according to the equation:

$$V = \left(A_v f_v j_d\right)/S. \tag{6}$$

where: A_v is total cross sectional area of vertical stirrups

f_v is allowable stress in the stirrups

j_d is internal moment arm.

S is spacing of stirrups in the direction of the axis of the member.

Ritter's ideas were not widely accepted at that time, but his design for vertical stirrups is similar to that appearing in the design specifications of most countries today [23].

In the web of reinforced concrete beams, Taylor [24] specifically mentioned to the point that inclined cracks are prevented from spreading by using transversal reinforcements such as stirrups. Practically, shear reinforcement takes three forms: stirrups, inclined bent up bars, or a combination of both. However, in industry, vertical stirrups are most commonly used because of their simplicity in fabrication and installation [25] as shown in Fig. 1.

Figure 1. Vertical Stirrups Reinforcements [7].

In addition to a citation issued by ACI-ASCE Committee 445 [26], many earlier tests were carried out by Zwoyer and Seiss [27] then by Moody and al. [28] confirming that the vertical shear stirrups (V_s) intercept diagonal cracks, and the nominal shear stress in steel is limited to:

$$V_s \leq 8\sqrt{f_c'}. \tag{7}$$

This limitation was also approved later on by Xu and al. [29] and by Morsy and al. [30].

An inverted-U shaped reinforcing assembly sample (called Hairpin) was primarily conducted by Abou Saleh and Suaris (2007) [6]. Such a system is shown in Fig. 2.

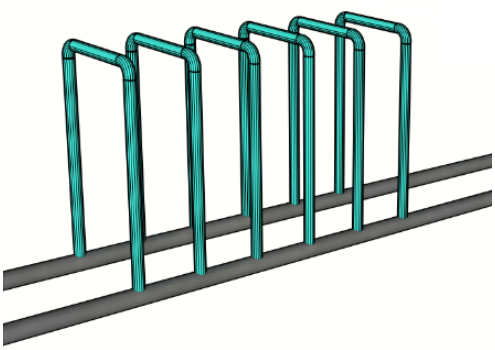

Figure 2. Inverted-U Shaped Reinforcements [7].

The use of such system improve experimentally the structural performance for an unbonded post-tensioned flat slab. The tested post-tensioned slabs provided with studs failed in pinching shear and the slabs provided with “Hairpin” shaped reinforcement failed in flexural. The test results with the stud reinforcement were almost equal to those predicted by the ACI equation. The slab with hairpin shaped reinforcement prevented the shear failure and showed about 27.5 % increase in slab capacity in comparison with the stud reinforcement [6].

According to the previous results, a proposed finite-element model was suggested in order to test the capability into predict the load–deflection relationships of the unbonded post-tensioned reinforced concrete slabs using finite element software. The outcomes of the conducted finite element analysis, utilizing ABAQUS software for the “Unbonded post-tensioned reinforced concrete slab provided with inverted U-shaped reinforcement”, are in line with that obtained experimentally, also the nominal shear strength that was compared to ACI provisions [17].

Recently, Khatib and Abou Saleh (2020) performed an experimental investigation for the enhancement of shear strength of bonded PTB provided with inverted-U shaped reinforcements [7]. The test results were compared with bonded PTB reinforced with conventional stirrups and correlated the results according to ACI provision.

The results indicate that the nominal shear stress (V_n) in bonded PTB provided with inverted-U shaped and stirrups reinforcements are respectively 14.4 $\sqrt{f_c'}$ psi (1.2 $\sqrt{f_c'}$ MPa) and 12.72 $\sqrt{f_c'}$ psi (1.06 $\sqrt{f_c'}$ MPa), which gives approximately 13 % increase in shear strength. Notice that no failure occurs in the welding due to its high proficiency and effectiveness.

Part of this paper presents the results of an experimental investigation for both the bonded PTB with inverted-U shaped and stirrups reinforcements [7]. These results were compared to the same model using a finite element software ANSYS 16.0 [31].

The primary goal of this research was to conduct a numerical evaluation of the shear strength behavior of bonded PTB with stirrups on one side and inverted-U shaped reinforcements on the other. The beams were also analyzed to compare the results to those obtained experimentally.

The aim of the study was to investigate the advantage of an inverted-U shaped system over a conventional one. The numerical model was used to correlate between the experimental results with those obtained numerically to give the proposed system a proper and absolute validity.

Recently, an experimental investigation for the improvement of shear strength of bonded PTB provided with inverted-U shaped reinforcements was conducted against other bonded PTB with stirrups reinforcements. The dimensions, pre-stressing strands, and shear reinforcements of the beams were chosen to yield a nominal shear stress of that is equivalent to 1.25 $\sqrt{f_c'}$, which approximately corresponds to an 18 % increase in shear strength. This increase is higher than that presented by the ACI for conventional reinforcements [7].

The test results indicate that the failure load for the inverted-U shaped specimens were slightly below the expected load (83 tons), which would ensure a shear failure mode of the bonded PTB [7]. According to ACI 318 [22], the beams were designed to ensure shear failure by checking that the obtained load from shear is less than that obtained due to bending. The tests were conducted by applying two concentrated point loads on the bonded PTB as shown in Fig. 3.

Figure 3. Tested Bonded Post-Tensioned Beam [7].

The concrete compressive strength applied was equal to 30 MPa. The seven prestressing wire strands conforming to ASTM standards A421 were 12.7 mm in diameter and at a specified ultimate strength of 1860 MPa.

The inverted-U shaped and stirrups reinforcements were fabricated using 10 mm diameter rebar that yielded a specified strength of 420 MPa. The distribution of the rebar and shear reinforcements are as shown in Fig. 4.

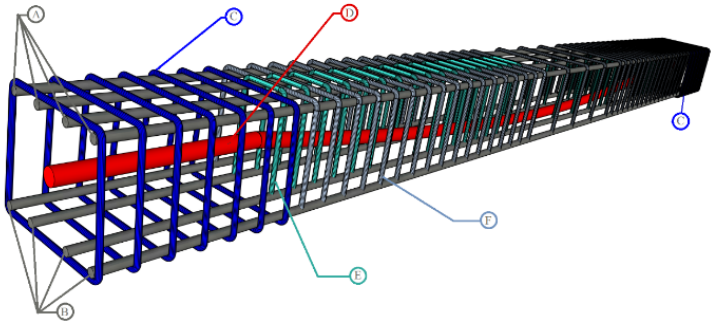

(a) Arrangement of Inverted-U Shaped Reinforcements and Rebars

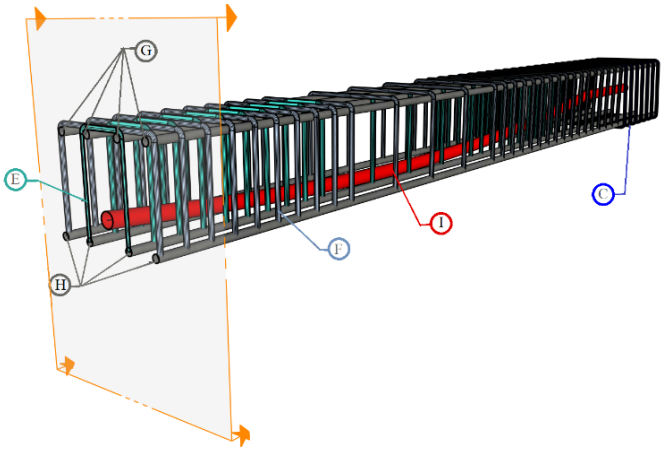

(b) Cross-Section for the Inverted-U Shaped Reinforcements.

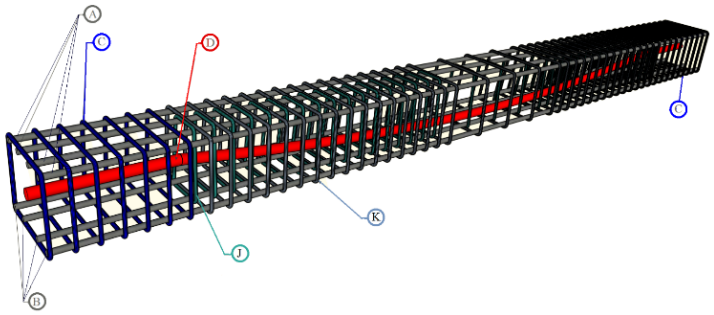

(c) Arrangement of Closed Stirrups Reinforcements and Rebars

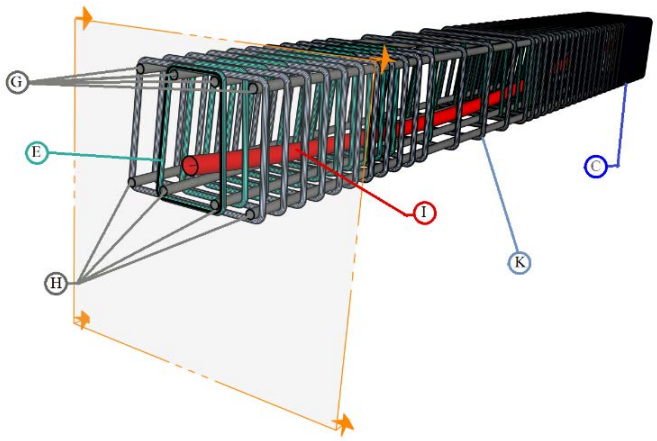

(d) Cross-Section for the Closed Stirrups Reinforcements

Figure 4. Arrangement of Shear Reinforcements and Reinforcements [7]
Where A: Top Rebars, B: Bottom Rebars, C: Steel Cage, D: Strands, E: Internal Inverted-U, F: External Inverted-U, G: Cross-Section in Top Rebars, H: Cross-Section in Bottom Rebars, I: Cross-Section in Strand, J: Internal Stirrups, K: External Stirrups.

In general, all tested specimens failed in shear mode. The experimental results were presented in Table.1.

Table 1. The experimental shear test results compared with ACI provision.

Specimen Designation	Test results				ACI Equation
	Failure loads Kips/ kN	Average failure load Kips/kN	Spacing between point Load in/mm	Nominal shear stress. Psi/MPa	Nominal shear stress Psi/MPa
PTB-A-1	187.98/836.2	181.92/ 809.24	47.24/1200	$14.40\sqrt{f_c'}$ /$1.20\sqrt{f_c'}$	N. A.
PTB-A-2	175.86/782.30		43.3/ 1100		
PTB-B-1	166.31/739.80	166.79/ 714.96	47.24/1200	$12.7\sqrt{f_c'}$ /$1.06\sqrt{f_c'}$	$10.8\sqrt{f_c'}$ /0. $9\sqrt{f_c'}$
PTB-B-2	155.14/690.11		43.3/1100		

These results indicate that the nominal shear stress in inverted-U shaped and stirrups reinforcements are respectively $14.4\sqrt{f_c'}$ psi ($1.2\sqrt{f_c'}$ MPa) and $12.72\sqrt{f_c'}$ psi ($1.06\sqrt{f_c'}$ MPa), which yield an approximate 13 % increase in shearing strength [7].

Good correlations exist between the designed and the actual experimental results. Furthermore, the test results indicate that the failure load of the inverted-U shaped specimens were a little below the expected load; thus, resulting in a shear failure mode of the bonded PTB.

Moreover, the average load deflection curves for the two types approve that the obtained results concerning the use of the inverted-U shaped reinforcements are better than those provided with the conventional closed stirrups reinforcements as shown in Fig. 5 [7].

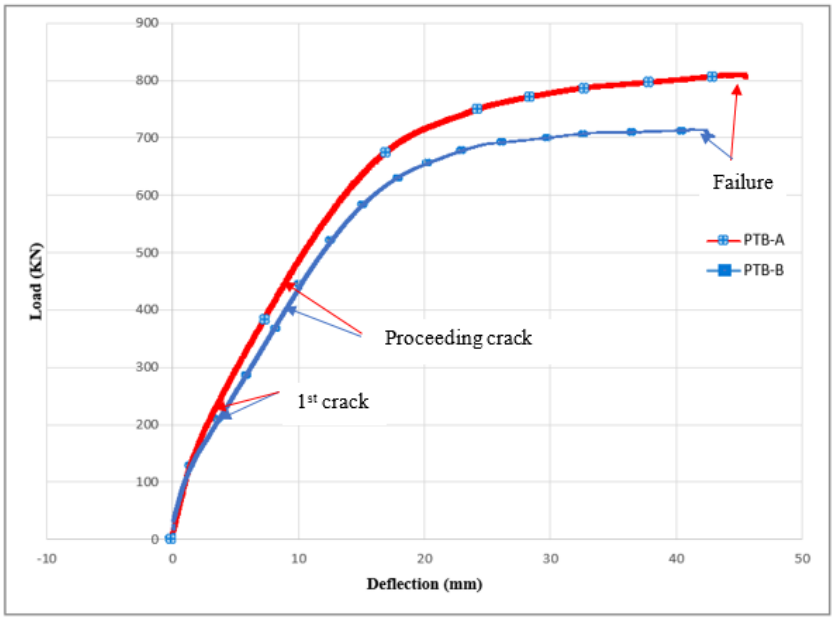

Figure 5. Load Deflection Curves for PTB – A & PTB – B (Average Values) [7].

The post-cracking stiffness is an important parameter in determining the proper distribution of forces in the analysis of PTB. It can be calculated as the triangular area under load deflection curve (linear elastic region). Although, different parameters can affect the energy absorption values, such as concrete compressive strength and steel reinforcement ratios, the energy absorption can be considered as the total area under the load deflection curve.

Refer to Fig. 5 both of post cracking stiffness and energy absorption for PTB-A show an effective enhancement comparing to PTB-B as shown in Table 2.

Table 2. The experimental enhancement results.

Specimen Designation	Average failure load Kips/kN	Nominal shear stress Psi/MPa	Post-Cracking Stiffness	Energy Absorption
PTB-A	181.92/809.24	$14.40\sqrt{f_c'}$ /$1.20\sqrt{f_c'}$	45.96	252.66
PTB-B	166.79/714.96	$12.7\sqrt{f_c'}$ /$1.0\sqrt{f_c'}$	41.88	207.48
% Enhancement	9.07%	13.4 %	9.75 %	21.77 %

2. Methods

Ever since the finite element was first introduced by Ngo and Scordelis (1967) [32] and applied to the analysis of reinforced beams, a huge number of methodologies for modeling the behavior of concrete as a material or the behavior of reinforced concrete structures have been established.

The obtained experimental results [7], mentioned earlier, were compared with the same model using a finite element software “ANSYS 16.0” [31]. The objective of this comparison is to validate the experimental results and highlight the effectiveness of the proposed system. Moreover, the modeled beams were analyzed to compare the obtained experimental test results.

The ANSYS 16.0 program [31] is capable of simulating structural analysis problems in a wide range of engineering disciplines, deformations, stresses, strains, and reaction forces. The analysis of a structure with ANSYS 16.0 is performed through the following pre-processing steps: The first process is defining the finite element model and the environmental factors applied to it. The second is analyzing the solver which

is the solution of the finite element model and finally post-processing the results like deformations, contours for displacement, etc…, using visualization tools.

An approach to modeling bonded PTB will usually aid in making better and improved engineering decisions about preparing the geometry, which includes beams, cables, reinforcement rebar, inverted-U shaped and stirrups reinforcements.

The finite element analysis calibration study included modeling bonded PTB with the dimensions and properties. In order to model them using ANSYS 16.0, there are multiple tasks that have to be completed for it to run properly. Models can be presented using either a command prompt line input or a Graphical User Interface.

For this model, the graphical user interface was utilized. This section describes the different tasks and entries used to model the finite element calibration. The boundary conditions and load application were identical to those used in the tests.

The main evaluation for a theoretical model is testing two types of bonded PTB: PT-1 (provided with inverted-U shaped reinforcements) and PT-2 (provided with stirrups reinforcements). Both types are analyzed using ANSYS 16.0.

The PTB was designed following the recommendations of PTI (Post Tensioning Institute) manual, so the profile of the strands is a fixed parameter and cannot be changed, because the profile was chosen to ensure the maximum benefit from the post-tension system. Concerning the level of force, in this study, it does not make any sense to change it. Since during the experimental tests, it was chosen the level to ensure the maximum efficiency force. However, the concrete compressive strength was changed to study its effect on the PTB.

2.1. Modeling of post-tensioned beams

The model is considered vertically symmetrical at mid span as performed in the previous test. The test specimens were 3.4 m × 0.3 m × 0.25 m. The concrete beam was modeled by drawing the area into the YZ plan and extruding it into the X direction as shown in Fig. 6.

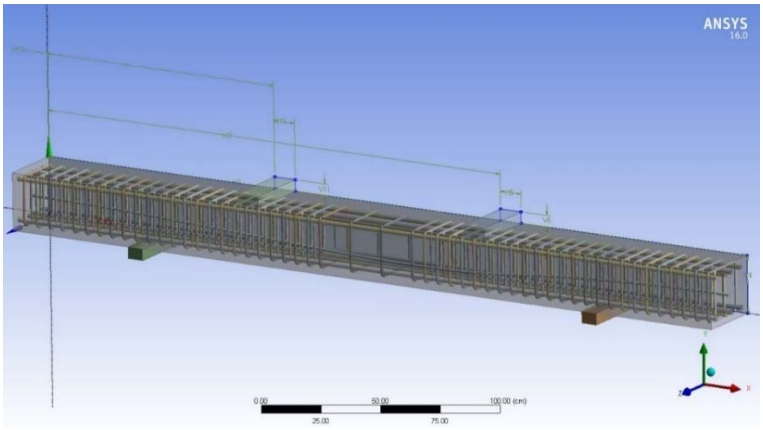

Figure 6. Modeling of PTB.

The element is a 10-node element model with a higher 3D order (SOLID187) as shown schematically in Fig. 7.

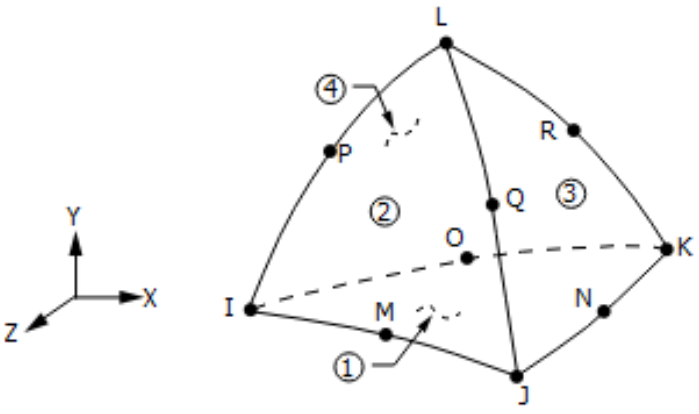

Figure 7. Solid 187 Element Model.

It has a quadratic displacement behavior and is well suited to modeling irregular meshes (such as those produced from various CAD/CAM systems). This element had three degrees of freedom at each node: translations in the nodal x, y, and z directions. The element has plasticity, hyperelasticity, creep, stress stiffening, large deflection, and large strain capabilities.

It also has a mixed formulation capability for simulating deformations of both partially incompressible elastoplastic materials and fully incompressible hyper-elastic ones. The element is capable of plastic deforming, cracking in three orthogonal directions, and crushing.

Four longitudinal reinforcements of 20 mm in diameter were placed at the top and bottom of the concrete beams as described before in the experiment investigation (Fig. 8).

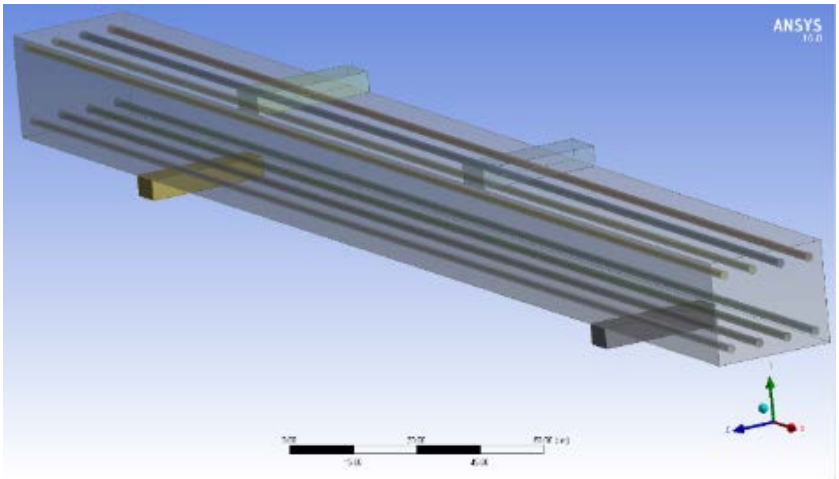

Figure 8. Rebar in Bonded PTB.

The shear reinforcements were located at the supports (max. shear region) of the beam, around the loaded or reaction area. Sixteen inverted-U shaped reinforcements of dimensions (21 cm×26 cm×21 cm) along with another sixteen of dimensions (21 cm×8 cm×21 cm) were used in the first beam type PT-1 as shown in Fig. 9.

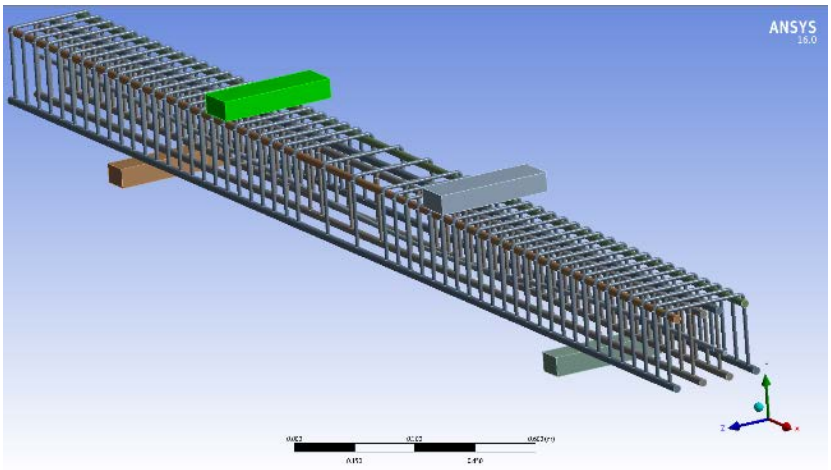

Figure 9. Inverted-U Shaped Distribution in Bonded PTB.

Also, another 16 closed stirrups reinforcements of dimensions (21 cm×26 cm) plus 16 closed stirrups reinforcements of dimensions (21 cm × 8 cm) were prepared for the second type of beam (PT-2) as shown in Fig. 10.

One sector was provided into the XZ plane in a longitudinal direction to model a cable. The cable geometry was entered with a curvilinear body and anchored at the ends through a thin cylindrical joint as shown in Fig. 11.

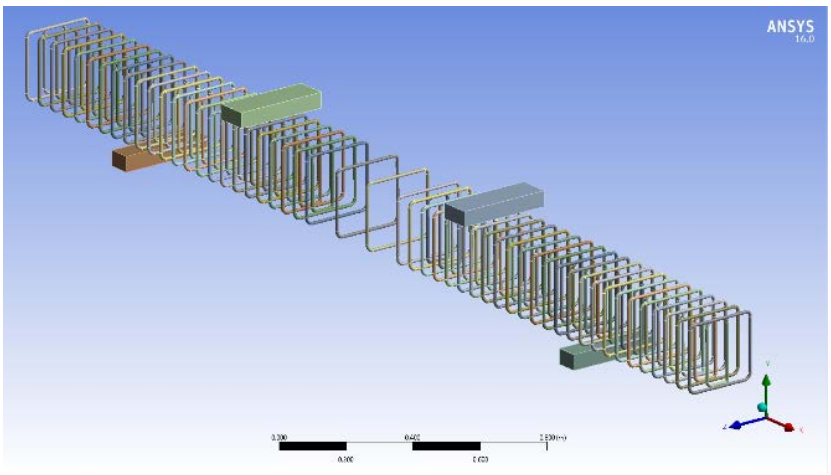

Figure 10. Stirrups Distribution in Bonded PTB.

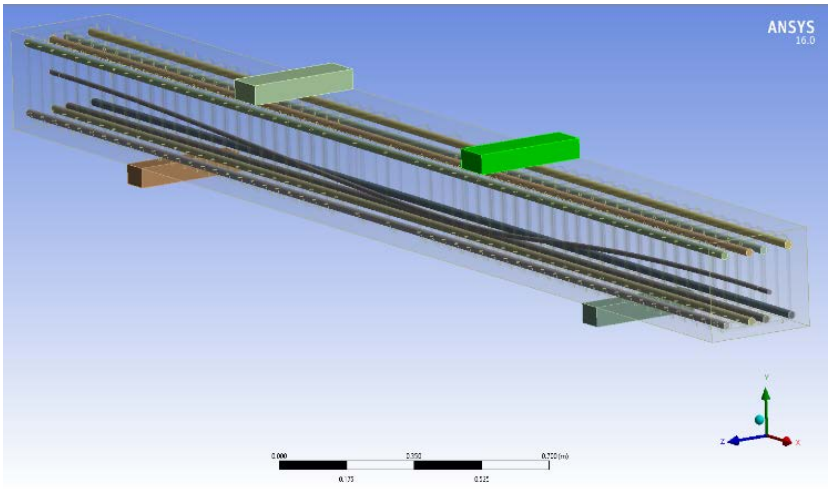

Figure 11. Layout of Post-Tensioned Cable.

2.2. Modeling of material properties

The material properties adopted for the discrete model concerning concrete, rebar steel, shear reinforcements (inverted-U shaped and stirrups reinforcements) used were taken from the accomplished experiments.

Concrete is modeled with the help of a solid element, SOLID186. In tension, the stress–strain curve is thus presumed to be linear elastic until it reaches the uniaxial tensile strength of the concrete. Thus, the concrete element eventually cracks.

By default, there is a model for concrete, but for the nonlinear analysis purpose, the plastic behavior model should be added. The simple one is the bilinear kinematic hardening model. But in order to get a better performance, the multilinear model is used and the values as stress-strain relationship are added as shown below in Table 3 and Fig. 12. The other concrete material values are listed in Table 4.

Table 3. Concrete stress strain values.

Plastic Strain	Stress (MPa)
0	1E-09
0.0006	15
0.0009	21.08
0.0012	25.27
0.0015	27.96
0.0018	29.42
0.0021	29.96
0.00219	30
0.003	30

Table 4. Concrete properties.

Properties	Values
Young's Modulus	25000 Mpa
Poison's ratio	0.1
Tensile Yield Strength	3.42 MPa

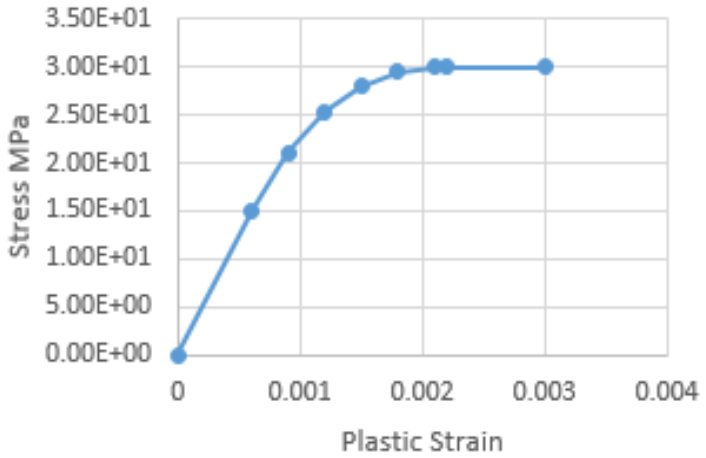

Figure 12. Stress-Strain Relationship for Concrete.

ANSYS 16.0 supplies a huge number of material libraries. Structural steel is one of them. The values were modified so that it would be similar to that used in the experimental analysis then added a plastic behavior model for the nonlinear analysis as listed in Table 5 by using the simpler one which is the bilinear isotropic hardening model. The values for yielding strength (420 MPa) and tangent modulus (6700 MPa) are added as shown in Fig.13.

Table 5. Rebars Properties.

Properties	Values
Young's Modulus	1.96*105 MPa
Poison's ratio	0.28
Tensile Yield Strength	420 MPa
Tangent Modulus	6700 MPa
Tensile Ultimate Strength	525 MPa

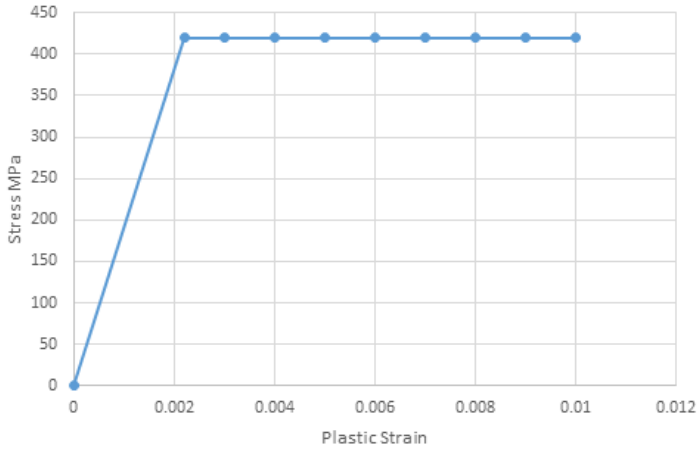

Figure 13. Stress-Strain Relationship for Steel.

The steel element model in the "Engineering Data Sources" was duplicated and renamed it as prestressed cables. The values were modified to have the same material properties used in the experimental analysis as shown in Table 6.

Table 6. Prestressed Cables Properties.

Properties	Values
Young's Modulus	2*105 MPa
Poison's ratio	0.3
Tensile Yield Strength	

2.3. Meshing

The Solid186 element was used to mesh the PTB. This properly sets width and length of the elements in the rebar and lets the cables be consistent with the elements and nodes in the concrete portions of the model. The necessary element divisions are noted. The model was meshed as shown in Fig. 14 using "Curvature" option in "Advanced size function", "Coarse" option for "Relevance Center with Medium Smoothing" and "Fast Transition" so that both the rebar and concrete elements share the same nodes. The same goes for cables and concrete.

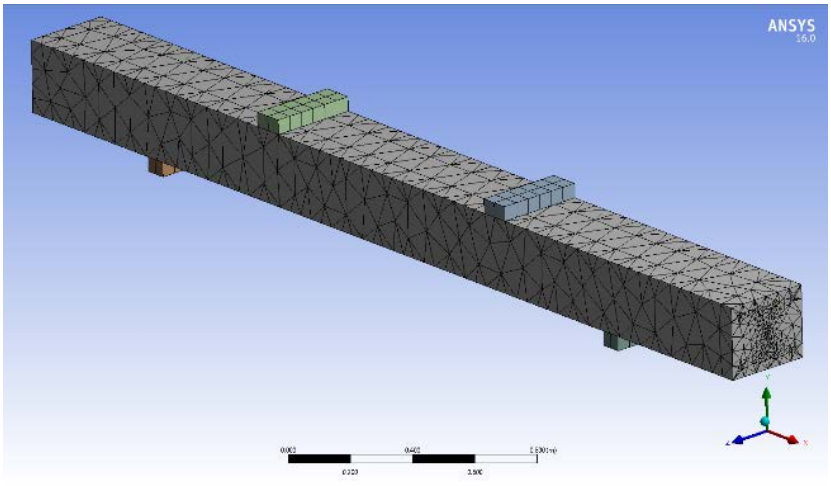

Figure 14. Meshed Bonded PTB.

An internal closed view for the meshed inverted-U shaped reinforcements and post-tensioned cables was shown in Fig. 15.

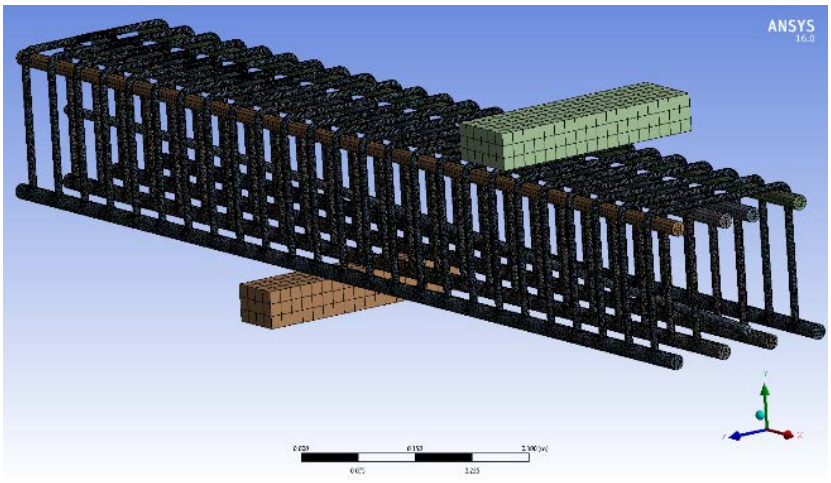

Figure 15. Internal Closed Meshed View for PT-1.

Another internal view for the meshed stirrups and post-tensioned cables was presented in Fig. 16.

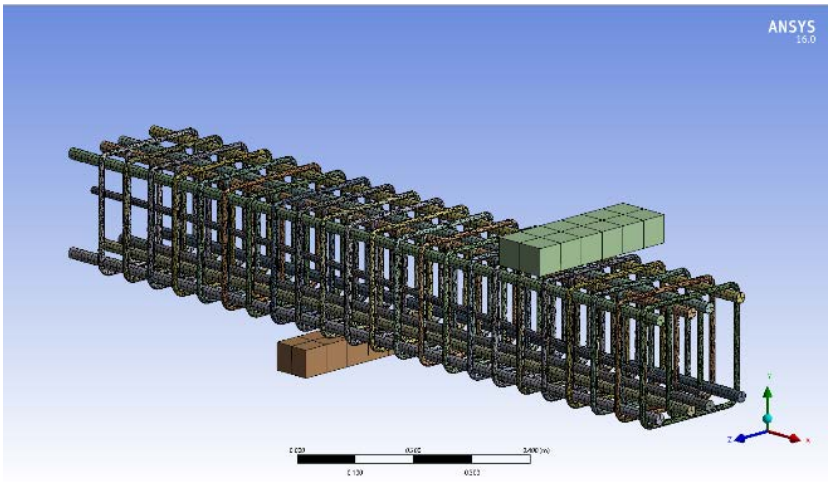

Figure 16. Internal Closed Meshed View for PT-2.

2.4. Loads and boundary conditions

The load was applied downwards at two separated points 30 cm from the center of the PTB. Two other different points, which were 200 cm apart from each other, were used to be the supports of the PTB. The beam also had a 70 cm overhanging on each side as shown in Fig. 17.

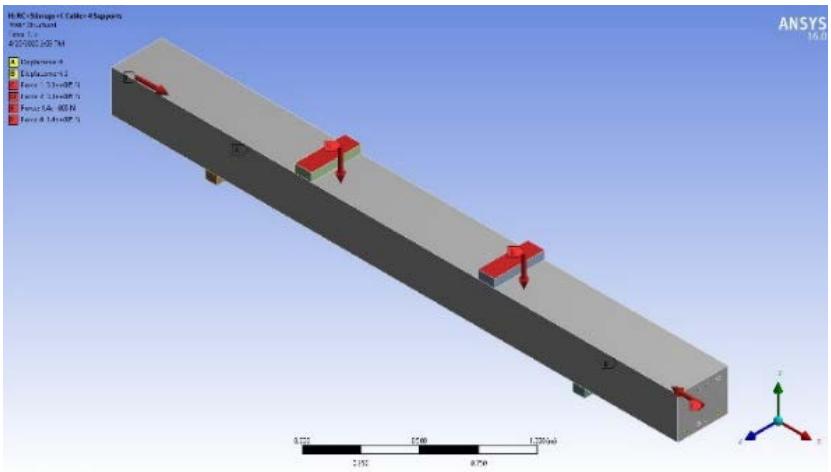

Figure 17. Bonded PTB Loaded.

3. Results and Discussion

The Analysis Settings was specifying to ON for the Large deflection and the numerical analysis started running. Numerical results of shear behavior of bonded PTB with inverted-U shaped and stirrups reinforcements were presented in this paper. These results state that both models failed in shear.

The initial cracking of the PTB provided with inverted-U (PT-1) appeared at a load P = 198 kN and the corresponding deflection is 3 mm. Smooth graded crack occurs as more load is applied to the PT-1. The second crack appeared at a load P = 431 kN with corresponding deflection equal to 8.5 mm. Thus, larger deflection takes place at mid-span, and the successive appearance cracking of the PT-1 means that significant cracks appear at beyond yielding of steel reinforcement. At 845.16 kN the PTB is at the verge of failure i.e. the cracking extends towards the top and record a deflection equals to 46 mm.

From X–Y plot results in Fig. 18 and the directional deformation colored contour bands for the PTB shown in Fig. 20. a,b a smooth graded crack occurred as the load increased and up to a 198 kN, the linear elastic material behavior for both steel reinforcement and concrete defines the flexural rigidity. When concrete stresses exceed modulus of rupture, cracked transformed moment of inertia in addition to linear elastic steel and concrete behavior defines the flexural rigidity of the beam, then the nonlinear concrete behavior takes place, at this stage deflection was computed based on curvature.

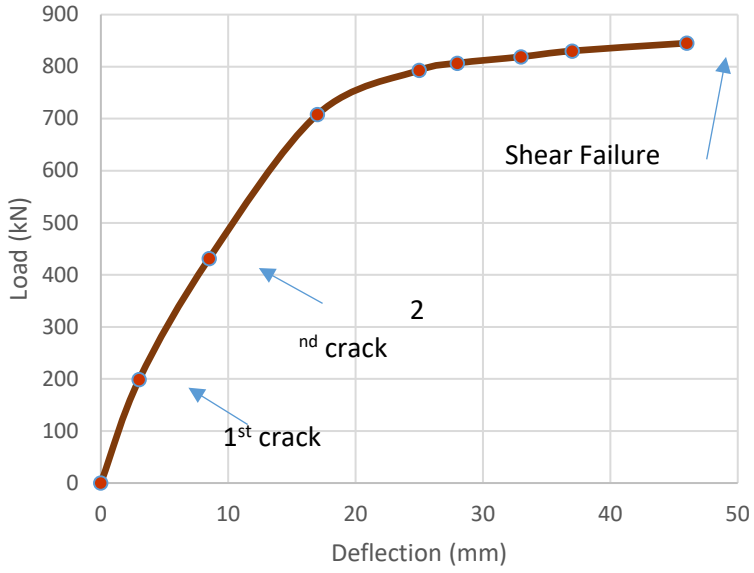

Figure 18. Load Deflection Curves for Numerical PTB (PT-1).

From the results obtained (Fig. 19) the bonded post-tensioned reinforced concrete beam provided with closed stirrups (PTB-2) crack initially at a load P = 200 kN with a corresponding deflection equals to 3.2 mm. It is noticed that at P = 400 kN the cracks develop in a sudden way caused a 9.5 mm as deflection, this implies that the tensile stress relaxation is not functioning properly. Cracking increases and the maximum load reached P = 756.20 kN caused a crushing in the top of the PTB model with deflection equals to 49.1 mm.

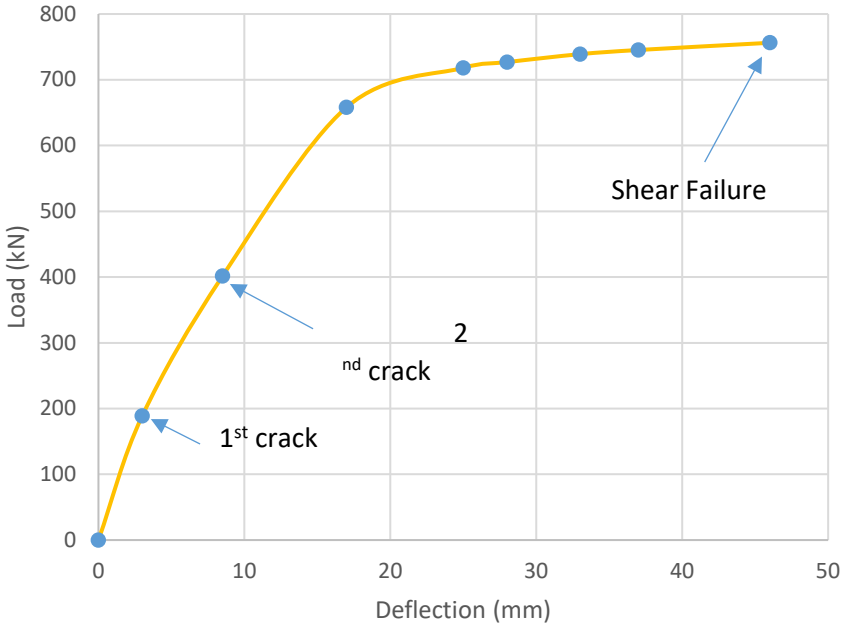

Figure 19. Load Deflection Curves for Numerical PTB (PT-2).

In order to investigate numerically the effect of the concrete compressive strength $\left(f_c'\right)$ on the two types of PTB (PT-1 & PT-2), several values were also studied (35 MPa, 40 MPa, 45 Mpa and 50 MPa). It was very clear, for both cases of PTB (PT-1 & PT-2) that with the increase of $\left(f_c'\right)$, the shear failure reach a higher value than the previous one as shown in Fig. 20.

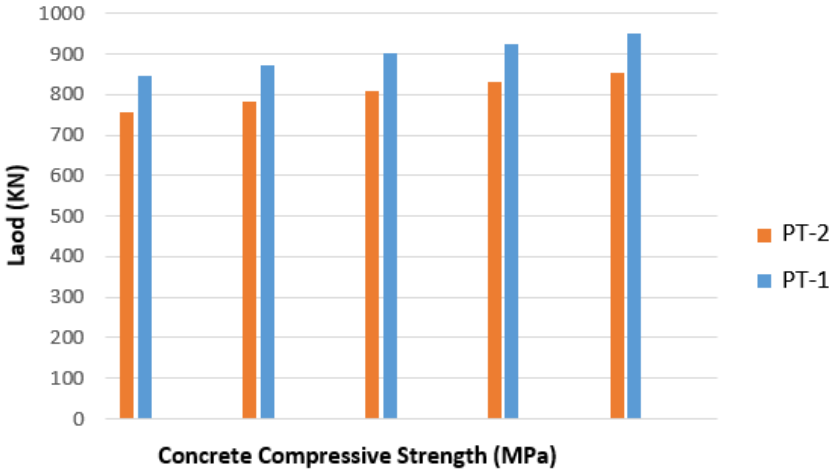

	30	35	40	45	50
PT-1	845.16	873.54	900.62	926.22	950.14
PT-2	756.20	781.60	807.85	830.80	852.26

Figure 20. Load-Concrete Compressive Strength Relationship.

The directional deformation results appear as colored bands on the two types of bonded PTB (PT-1 & PT-2) as shown in Fig. 21.

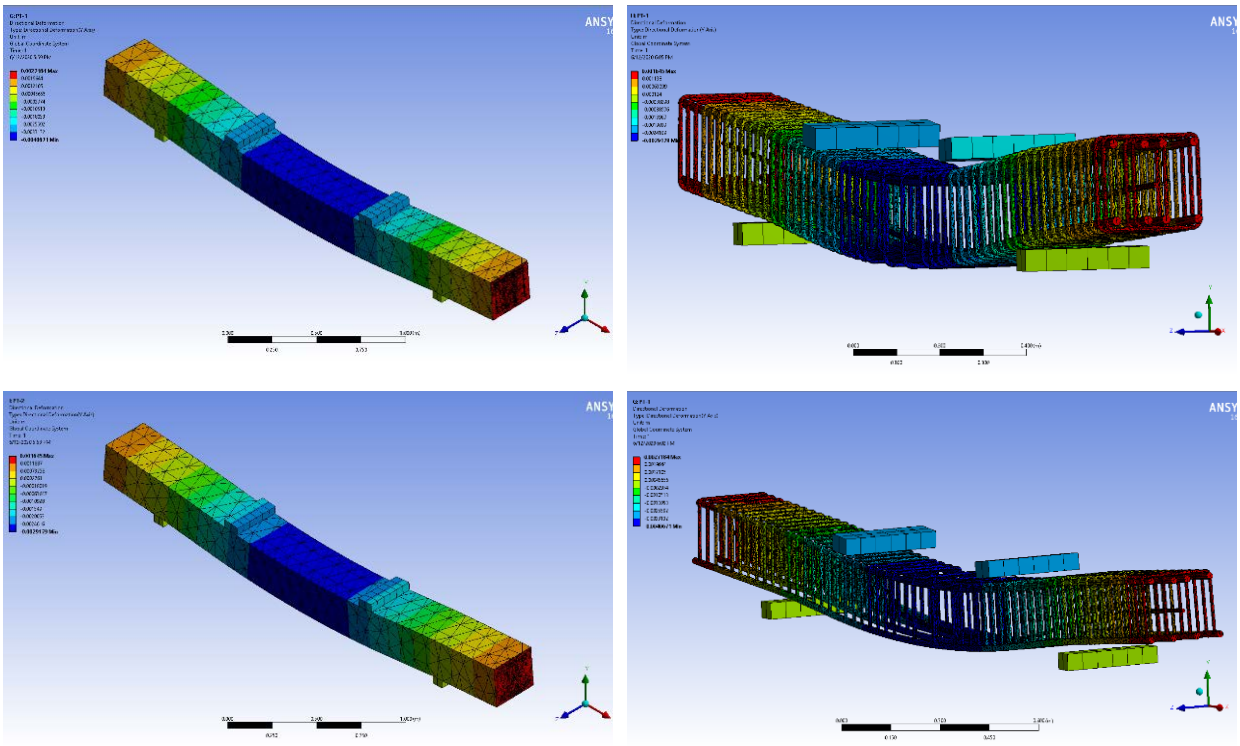

Figure 21. Top-left: Last Directional Deformation Beam Colored Bands for PT-1; Top-right: Internal View for Last Directional Deformation Colored Bands for PT-1; Bottom-left: Last Directional Deformation Beam Colored Bands for PT-2; Bottom-right: Internal View for Last Directional Deformation Colored Bands for PT-2.

The numerical results of bonded PTB with shear stirrups were almost equal to those predicted by the ACI equation. The comparisons were made between load deflection curves at mid-span and failure load. The results of the finite element analysis were calculated at the same location as the experimental test of the beams.

The bonded PTB capacity with the inverted-U shaped reinforcements was about 11.76 % higher than the bonded PTB with the stirrups. An enhancement was observed in the ductility computed as the

percentage difference in the max deflection between the two beams. The numerical results have shown that the use of inverted-U shaped reinforcements structurally behave as good if not better as shear reinforcements than stirrups do.

The accuracy of the finite element models was assessed by comparison with the experimental results that appear to be in good agreement. The load-deflection curves from the finite element analysis agree well with the experimental results in the linear range till peak load as appears in Table 7 and Fig. 22.

Table 7. Comparison of Numerical and Experimental PTB Results with ACI Provision.

Specimen designation	Average failure load Kips/ kN	Test Results Nominal shear stress psi /MPa	ACI Equation Nominal shear stress psi /MPa
PTB-A	181.92/ 809.24	$14.40\sqrt{f_c'}$ /$1.20\sqrt{f_c'}$	N. A.
PTB-B	166.79/ 714.96	$12.72\sqrt{f_c'}$ /$1.06\sqrt{f_c'}$	$10.8\sqrt{f_c'}$ /$0.9\sqrt{f_c'}$
Numerical Results			
PT-1	190 / 845.16	$15.04\sqrt{f_c'}$ / $1.25\sqrt{f_c'}$	N. A.
PT-2	170 / 756.20	$12.96\sqrt{f_c'}$ / $1.10\sqrt{f_c'}$	$10.8\sqrt{f_c'}$ /$0.9\sqrt{f_c'}$

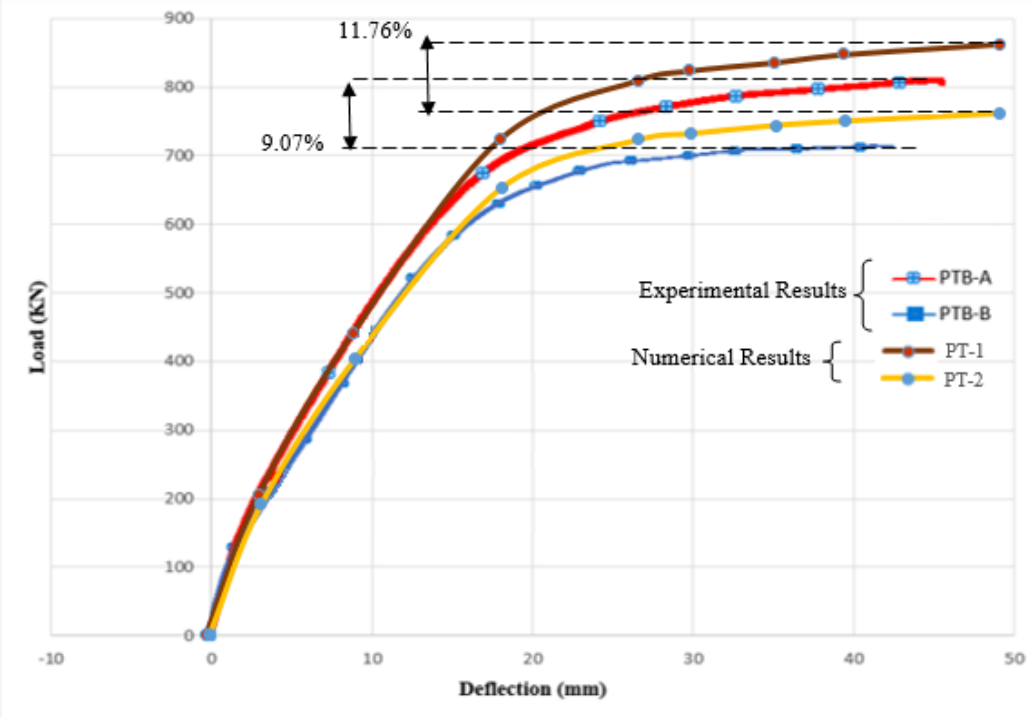

Figure 22. Load Deflection Curves for Experimental PTB (PTB-A and PTB-B) and Numerical PTB (PT-1 and PT-2).

The obtained numerical results show improvement values as much the experimental ones. The percentage enhancement concerning Average load failure, Nominal shear stress, Post-Cracking Stiffness and Energy Absorption were shown in Table 8.

Table 8. Comparison of Enhancement for Numerical and Experimental PTB Results.

Specimen Designation	Average failure load Kips/ kN	Nominal shear stress psi /MPa	Post-Cracking Stiffness	Energy Absorption
Test Results				
PTB-A	181.92/ 809.24	$14.40\sqrt{f_c'}$ /$1.20\sqrt{f_c'}$	45.96	252.66
PTB-B	166.79/ 714.96	$12.72\sqrt{f_c'}$ /$1.06\sqrt{f_c'}$	41.88	207.48
%Enhancement	9.07 %	13.4 %	9.75 %	21.77 %
Numerical Results				
PT-1	190/845.16	$15.04\sqrt{f_c'}$ /$1.25\sqrt{f_c'}$	57.28	275.25
PT-2	170/756.20	$12.96\sqrt{f_c'}$ /$1.10\sqrt{f_c'}$	52.87	229.56
%Enhancement	11.76 %	16.04 %	8.34 %	19.90 %

The numerical results give values higher than the experimental ones; however, the properties of concrete during the achieved experiments were possibly not as similar as estimated. According to the numerical results obtained, the proposed finite element model proves the capability to accurately predict the load deflection relationships of the bonded PTB. To obtain new equations governing the design of inverted-U shaped reinforcements, further research is needed.

4. Conclusion

A nonlinear finite element model, ANSYS 16.0, was developed and presented for the analysis of two bonded PTB. The first was provided with inverted-U shaped reinforcements while the second was provided with closed stirrups reinforcements. The interface between the tendon and the surrounding concrete was modeled allowing the tendon to retain its profile shape during the deformation of the beam. The comparison between the experimental and numerical results showed that the model can predict the behavior of bonded PTB. The numerical results allow to draw following conclusions:

1. The outcomes of the conducted finite element analysis, utilizing ANSYS 16.0 software for the bonded PTB provided with inverted-U shaped and stirrups reinforcements are in good agreement in terms of load deflection relationship with that obtained experimentally.

2. Structural modeling using SOLID187 finite element utilizing ANSYS 16.0 software properly simulate the behavior of bonded PTB provided with inverted-U shaped and stirrups reinforcements.

3. It was planned that the testing results should give values higher than the numerical ones; however, the properties of concrete during the testing process were perhaps not as homogenous as expected.

4. The numerical model of bonded PTB provided with inverted-U shaped reinforcements failed in shear mode with an increase in capacity of about 11.76 % above the numerical model of bonded PTB provided with stirrups before collapsing.

5. The nominal shear stress for bonded PTB provided with inverted-U shaped reinforcement was equal to $1.25\sqrt{f_c'}$ MPa and could actually be as high as the bonded PTB provided with stirrups by 16.05 %.

References

1. Nawy, E.G. Prestressed Concrete: A Fundamental Approach (5th ed). Pearson/Prentice Hall, 2012. [Online].
2. Dunker, K.F. Strengthening of simple span composite bridges by post-tensioning [Iowa State University, Digital Repository], 1985. DOI: 10.31274/rtd-180813-13333
3. Garden, H.N., Hollaway, L.C. An Experimental Study of the strengthening of Reinforced Concrete Beams using Prestressed Carbon Composite Plates. Proceedings of 7th Int. Conf. Structural Faults and Repair. Edinburgh, 1997. V. 2. Pp. 191–199.
4. Abou Saleh, Z., Sauris, W. Reinforcing Assemblies and Reinforced Concrete Structures. Patent USA US20080263978A1, 2008.
5. Kang, T., Huang Y., Shin M., Lee J., Sir Cho A. Experimental and Numerical Assessment of Bonded and Unbonded Post-Tensioned Concrete Members. ACI Structural Journal. 2015. 112 (6). Pp. 735–748. DOI: 10.14359/51688194
6. Ellobody, E., Bailey, C. Behaviour of Unbonded Post-Tensioned One-Way Concrete Slabs. Advances in Structural Engineering Journal. 2016. 11(01). Pp. 107–120. DOI: 10.1260/136943308784069504

7. Xue, W., Tan, Y., Peng, F. Experimental Study on Damaged Prestressed Concrete Beams Using External Post-Tensioned Tendons. ACI Structural Journal. 2019. 117(1). Pp. 159–168. DOI: 10.14359/51718019
8. Khatib, M., Abou Saleh, Z. Enhancement of Shear Strength of Bonded Post-Tensioned Beams Using Inverted-U Shaped Reinforcements. Case Studies in Construction Materials Journal. 2020. Vol. 13. DOI: 10.1016/j.cscm.2020.e00370
9. Hrennikoff, A. Solution of Problems by the Frame Work Method. Journal of Applied Mechanics. 1941. 8(4). Pp.169–175.
10. Courant, R. Variational Methods for the Solution of Problems of Equilibrium and Variations. Bulletin of the American Mathematical Society. 1943. No. 49. Pp. 1–23.
11. Hampshire, J.K., Topping, B.H.V., Chan, H.C. Three Node Triangular Bending Elements with One Degree of Freedom per Node. Engineering Computations. 1992. 9 (1). Pp. 49–62. DOI: 10.1108/eb023848
12. Kim, H., Christopoulos, C. Numerical models and ductile ultimate deformation response of post-tensioned self-centering moment connections. Earthquake Engineering Structural Dynamic. 2008. 38(1). Pp. 1–21. DOI: 10.1002/eqe.836
13. Ellobody, E., Bailey, C. G. Modelling of Unbonded Post-Tensioned Concrete Slabs under Fire Conditions. Fire Safety Journal. 2009. Vol. 44. Pp. 159–167. DOI: 10.1016/j.firesaf.2008.05.007
14. Huang, Y., Kang, T.H.-K., Ramseyer, C., Rha, C. Background to multi-scale modelling of unbonded Post-Tensioned concrete structures. International Journal Theoretical and Applied Multiscale Mechanicsю 2010. 1(3). Pp. 219–235.
15. Kim, K.S., Lee, D. Nonlinear analysis method for continuous post-tensioned concrete members with unbonded tendons. Engineering Structures. 2012. 40 (1). Pp. 487–500. DOI: 10.1016/j.engstruct.2012.03.021
16. Kulkarni, A., Bhusare V. Structural optimization of reinforced concrete structures. International Journal of Engineering Research. 2016. 5 (07). DOI: 10.17577/IJERTV5IS070156
17. Khatib, M., Abou Saleh, Z., Baalbaki, O. Punching Shear Analysis of Bonded Post-Tensioned Slabs with Inverted-U Shaped Reinforcements. Proceedings 9th Alexandria International Conference on Structural and Geotechnical Engineering. AICSGE 9. Alexandria, 2016. Pp. RC 16-RC 17.
18. Mohammed, A. H., Abdul-Razzaq, K. S., Mohammedali, T. K., Nassani K., D. E., Hussein, A. K. Finite Element Modeling of Post-Tensioned Two-Way Concrete Slabs under Flexural Loading. Civil Engineering Journalю 2018. 4(1). DOI: 10.28991/cej-030964
19. Khatib, M., Abou Saleh, Z., Baalbaki, O., Temsah, Y. Numerical Punching Shear Analysis of Unbonded Post-Tensioned Slabs with Inverted-U Shaped. KSCE Journal of Civil Engineeringю 2018. 22(11). DOI: 10.1007/s12205-018-1505-5
20. Hawkins, N., Kuchma, D., Mast, R., Marsh, M.L., Reineck, K.-H. Simplified Shear Design of Structural Concrete Members: Appendixes, 2005. [Online] URL: https://onlinepubs.trb.org/onlinepubs/nchrp/nchrp_w78.pdf. (13.11.2020)
21. Słowik, M. The analysis of failure in concrete and reinforced concrete beams with different reinforcement ratio. Archive of Applied Mechanicsю 2019. 89 (5). DOI: 10.1007/s00419-018-1476-5
22. ACI Committee 318. Building Code Requirements for Structural Concrete (ACI 318-05) and Commentary (ACI 318R-05), 2005.
23. Report of ACI ASCE Committee 326 (now 426). Shear and Diagonal Tension, 2008. [Online] URL: https://www.scribd.com/document/340287092/Report-of-ACI-ASCE-Committee-326-Shear-and-Diagonal-Tension-Part-3-Siabs-and-Footings-Chapter-8-March1962 (13.11.2020)
24. Taylor, R. The Design Of Stirrups In Reinforced Concrete Beams. Architectural Science Review. 1964. 7 (3). DOI: 10.1080/00038628.1964.9696122
25. Al-Nasra, M., Asha, N. Shear Reinforcements in the Reinforced Concrete Beams. American Journal of Engineering Research. 2013. 2(10).
26. Muttoni, A., Fernández Ruiz, M., Simões, J.T. The theoretical principles of the critical shear crack theory for punching shear failures and derivation of consistent closed-form design expressions. Structural Concrete. 2018. 19(1). DOI: 10.1002/suco.201700088
27. Zwoyer, E.M., Seiss, C.P. Ultimate Strength in Shear of Simply-Supported Prestressed Concrete Beams Without Web Reinforcements. ACI Journal. 1954. 26 (2). Pp. 181–200.
28. Moody, K.G., Viest, M., Elstner, R.C., Hognestad, E. Shear Strength of Reinforced Concrete Beams – Part 1: Tests of Simple Beams. ACI JOURNAL. 1954. 51(4). Pp. 317–332.
29. Xu, S., Zhang, Z., Li, R., Qiu, B. Experimental Study on the Shear Behavior of RC Beams with Corroded Stirrups. Journal of Advanced Concrete Technology. 2017. 15(4). DOI: 10.3151/jact.15.178
30. Morsy, N.S., Sherif, A.G., Shoeib, A.E., Agamy, M.H. Experimental Study of Enhancing the Shear Strength of Hidden/Shallow Beams by Using Shear Reinforcement. 2018. DOI: 10.11159/icsenm18.116
31. ANSYS, I. Theory Reference for the Mechanical APDL and Mechanical Applications: Vol. Release 12, 2009
32. Ngo D., Scordelis A.C. Finite Element Analysis of Reinforced Concrete Beams. ACI Journal. 1967. No. 3. Pp. 152–163.

Contacts:

Milad Khatib, milad.khatib@isae.edu.lb

Zaher Abou Saleh, abousalehza@rhu.edu.lb

Oussama Baalbaki, obaalbaki@bau.edu.lb

Ziad Hamdan, ziad.hamdan.2@ul.edu.lb

Received 27.07.2020. Approved after reviewing 13.04.2021. Accepted 14.04.2021.